International Journal for Computational Civil and Structural Engineering, 21(1) 188–201 (2025)

DOI:10.22337/2587-9618-2025-21-1-188-201

STRENGTH ANALYSIS OF STEAM TURBINE BLADES FOR A NUCLEAR POWER PLANT

Patrick L. Kiprotich, Mariia V. Volkova, Robert F. Siro

National Research Nuclear University NRNU IATE MEPhI, Obninsk, RUSSIA

Abstract: The blade is an aerofoil-shaped component of a steam turbine that has a root attached to the rotor. The root is the base of the blade that supports the entire structure and transmits the torque generated by the steam flow to the rotor. The root must be designed in a manner that takes into account its removal during maintenance and positional maintenance on-the-fly during turbine operation. This essentially ensures a safe working environment for the operators and other personnel in the nuclear power plant.

Strength analysis of a steam turbine blade is a prerequisite procedure in the steam turbine design process during which the strength and durability of the blades under various operating conditions are evaluated. Such operating conditions include elevated temperatures, intense pressure and high rotational speeds. The purpose of this scientific work is to demonstrate that the blades can withstand such extreme conditions with little or no degradation over time. The adopted methodology involves modeling of the steam turbine blade using SolidWorks, and using the Finite Element Analysis (FEA) software to simulate the mechanical behavior of the associated blade material under various stress and strain conditions. The analysis takes into account factors such as stress distribution and concentration to predict the response of the blade under high pressure steam jets. The results of the analysis are adopted in the optimization of blade design and material selection to ensure safe and efficient blade operation throughout the entire lifespan of the turbine blade. The results are also useful in the identification of potential areas of weakness or failure that can be addressed through design changes and material improvements.

Keywords: Strength analysis, steam turbine blade, finite element analysis, SolidWorks, Ansys, static structural analysis, nuclear power plant

РАСЧЕТ ПРОЧНОСТИ ЛОПАТОК ПАРОВОЙ ТУРБИНЫ ДЛЯ АТОМНОЙ ЭЛЕКТРОСТАНЦИИ

П.Л. Кипротич, М.В. Волкова, Р.Ф. Сиро

Национальный исследовательский ядерный университет «НИЯУ ИАТЭ МИФИ», г. Обнинск, РОССИЯ

Аннотация: Лопатка является компонентом паровой турбины в форме аэродинамического профиля, который имеет корень, прикрепленный к ротору. Корень — это основание лопатки, которое поддерживает всю конструкцию и передает крутящий момент, создаваемый потоком пара, на ротор. Корень должен быть спроектирован таким образом, чтобы учитывать возможность его демонтажа во время обслуживания и сохранение его положения в процессе работы турбины. Это, по сути, обеспечивает безопасные условия труда для операторов и другого персонала на атомной электростанции. Анализ прочности лопатки паровой турбины является обязательной процедурой в процессе проектирования паровой турбины, в ходе которой оцениваются прочность и долговечность лопаток при различных условиях эксплуатации. К таким условиям относятся повышенные температуры, интенсивное давление и высокие обороты. Целью данной научной работы является демонстрация того, что лопатки могут выдерживать такие экстремальные условия с минимальным или отсутствующим ухудшением прочности со временем. Принятая методология включает моделирование лопатки паровой турбины с использованием Solidworks и применение программного обеспечения, использующего метод конечных элементов (FEA) для симуляции механического поведения связанного материала лопатки при различных условиях напряжения и деформации. Расчет учитывает такие факторы, как распределение напряжений и их концентрация, чтобы предсказать напряженно-деформированное состояние лопатки под воздействием струй пара под высоким давлением. Результаты расчета используются для оптимизации проектирования лопаток и выбора материалов, чтобы обеспечить безопасную и эффективную работу лопаток на

протяжении всего срока их службы. Результаты также полезны для выявления потенциальных зон слабости или отказа, которые могут быть устранены за счет изменения конструкции и улучшения материалов.

Ключевые слова: расчет на прочность, лопатка паровой турбины, метод конечных элементов, Solidworks, Ansys, статический расчет на прочность, атомная электростанция

1. INTRODUCTION

A steam turbine is a fundamental subsystem in every power generation complex, particularly in nuclear power plants in which they convert the potential energy stored in high pressure steam into kinetic energy associated with the rotating turbine blades, generating a rotary motion for driving electrical generators which ultimately results into electrical power. The efficiency and reliability of the turbine is critically dependent on the performance of the blades, which are subjected to extreme operating conditions associated with very high temperatures, pressures and rotational speeds. In this scientific work, we perform a strength analysis of the last-stage reaction-type steam turbine blades. Understanding the mechanical behavior of these blades under operational stresses is essential in preventing failures and ensuring the longevity of the turbine.

The primary objective of this scientific work is to model, analyze and validate the stresses associated with the steam turbine blade subjected to the extreme conditions formerly mentioned. In the analysis, it is assumed that the manifestation of such conditions is uniform on all the blades and so the results associated with a single blade can be replicated to give a whole picture of the condition of all the blades in the turbine. By conducting a detailed analysis of the impact of these conditions on the blade, we get results that are crucial in the enhancement of the design and material selection for the turbine blades.

By integrating advanced modeling and simulation techniques, the study provides a comprehensive understanding of the stresses manifesting on the turbine blades, a prerequisite stage in informed decision making on the basis of the adopted materials and design improvements. Additionally, the analysis procedure adopted in this scientific work can easily be applied in other types of turbines and components, contributing to the broader field of engineering and power generation. The findings in the study are expected to have practical implications in the maintenance and design of steam turbines, ultimately enhancing the stability and efficiency of power plants.

1.1 A Brief Description of the Steam Turbine Blade and the Investigated Conditions

A steam turbine operates under the fundamental principle of the Rankine Cycle, a thermodynamic cycle that transforms heat energy into mechanical work. In the Rankine cycle, high-pressure steam is generated in the steam generator. The steam is subjected to expansion in a series of turbine stages to create a rotary motion needed to facilitate the motion of conductive material through the magnetic field lines associated with permanent magnets of the electrical generator. The steam is then condensed and reintroduced into the cycle.

The blade causes the rotation of the rotor by the action of reactionary or impulsive forces when a jet of steam traverses over its surface. It's installed in slots on discs connected to a rapidly rotating shaft. The blade is engineered to allow steam to flow smoothly over its surface, altering direction and generating a force that induces rotary motion. In a nuclear power plant (NPP), the turbine operates at extreme conditions associated with high temperatures, oxidation, cavitation, corrosion, bending and centrifugal forces associated with the flowing steam, necessitating the selection of materials that can withstand such conditions. The design of the steam turbine blades must therefore take all these factors into consideration.

Materials such as INCONEL 718, a precipitation-hardened nickel-based superalloy, are capable of withstanding these conditions but require rigorous testing before use [1,2].

The blade consists of 3 main parts; the leaf type, the blade root, and the blade tip, normally mounted in a disc containing shaft as illustrated in figure 1 [3].

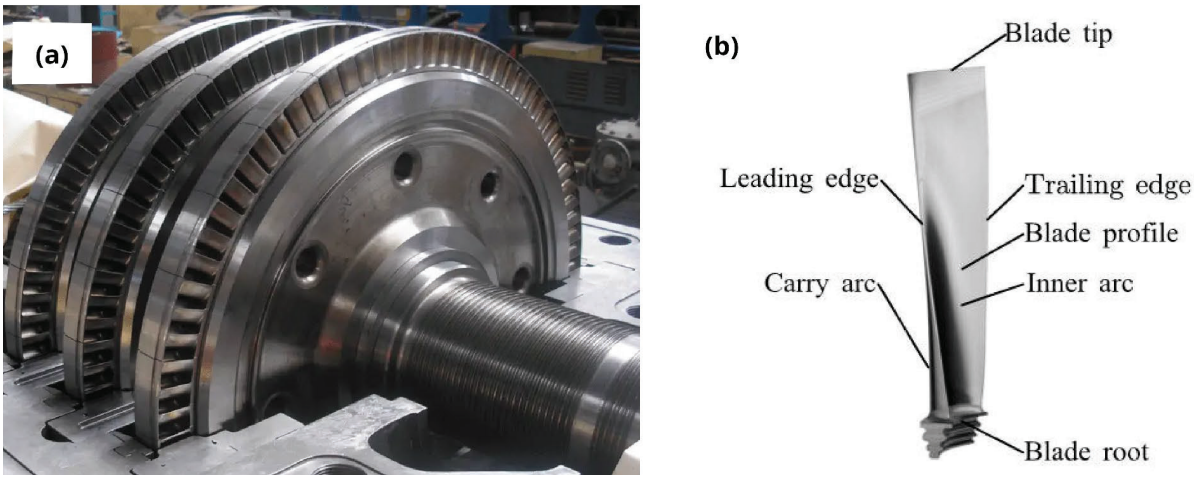

Figure 1. Turbine blades: (a) The shaft and disc with turbine blades, (b) Basic structure of a twisted blade

Each edge of a cross-section is referred to as a profile line, which, along with the section profile line and the leaf height parameters, adheres to gas dynamics requirements and ensures structural strength. Due to multi-axial stress state from the load, the blade must be modeled using 3-dimensional (3D) solid elements. The 3D model allows for detailed views of the maximum stresses, ensuring the design remains within safe limits. The blade's shape is determined by the minimum inertia of the section, while its strength and vibration performance are influenced by several aerodynamic parameters, including the impeller's suiting mode on the main shaft, the geometric inlet angle, and the exit angle [4].

1.2 Steam Turbine Blade Material Strength Analysis

Numerous studies have been conducted to analyze the strength and life expectancy of steam turbine blades under various loading scenarios. Researchers have employed a range of analytical, numerical and experimental techniques to investigate the complex stress distributions, material behaviors and failure mechanisms associated with these components.

Analytical methods, such as beam theory and energy methods, have been widely used to estimate the stresses and deformations in turbine blades subjected to centrifugal, thermal, and aerodynamic loads. These methods provide closed-form solutions and offer insights into the dominant failure modes, such as high-cycle fatigue, creep, and low-cycle fatigue [5].

Numerical techniques, particularly the FEA, have proven to be powerful tools for detailed stress analysis and turbine blade lifespan prediction. This method can incorporate complex blade geometries, material properties and loading conditions to accurately simulate the blade's structural response and identify critical stress concentration regions [6].

Experimental investigations have played a crucial role in validating analytical and numerical models, as well as understanding the underlying failure mechanisms. Static, fatigue, creep and thermal cycling tests have been conducted on actual blade specimens or scaled models to provide valuable data on material behavior, crack initiation and propagation, and

the effects of the environmental factors such as temperature and corrosion [7].
Strength analysis has led to the development of new alloys and coatings designed to enhance the strength and durability of turbine blades. Such materials exhibit superior high-temperature strength, creep resistance, and oxidation resistance, enabling longer service life and improved performance in nuclear power plant applications [8].
To achieve reliable performance, it is essential that the working stress manifesting on the turbine blades does not exceed the maximum allowable stress associated with the material.

1.3 Principles of Operation of Turbines

Turbines can be categorized based on the principle of their operation. In this case, we consider the categorization into impulse turbine and the reaction turbine. The impulse turbine operates by utilizing high-pressure steam that enters a stationary nozzle, consequently experiencing a decrease in pressure and a corresponding increase in velocity. The high-velocity steam is directed towards properly shaped turbine blades, generating an impulse force as it changes the steam flow direction upon impact. The resultant force instigates blade movement, initiating a rotary motion. The impulse turbine maintains a constant pressure across the moving blades. While the stationary nozzles facilitate a pressure drop and an increase in velocity, the moving blades do not experience any changes in pressure. On the other hand, the reaction turbine consists of rows of fixed and moving blades. Initially, the steam expands in the fixed blades, increasing in velocity while its pressure decreases. As the steam gets to the moving blades, its direction changes, creating an impulse force on the blades. While traversing through the moving blades, it continues to expand and its pressure further drops, generating a reaction force that drives the turbine. A key characteristic of the reaction turbine is the pressure differential between the inlet and the outlet of the moving blades, indicating a significant pressure drop across the blades [5].

2. MATERIALS AND METHODOLOGY

The adopted methodology entailed creation of the 3D model of the turbine blade using SolidWorks, adoption of the analytical computation scheme for the stress, adoption of the ANSYS supported numerical computation in simulating stress, and validation of results by comparing the adopted numerical and analytical computation models. The implementation workflow diagram is presented in figure 2.

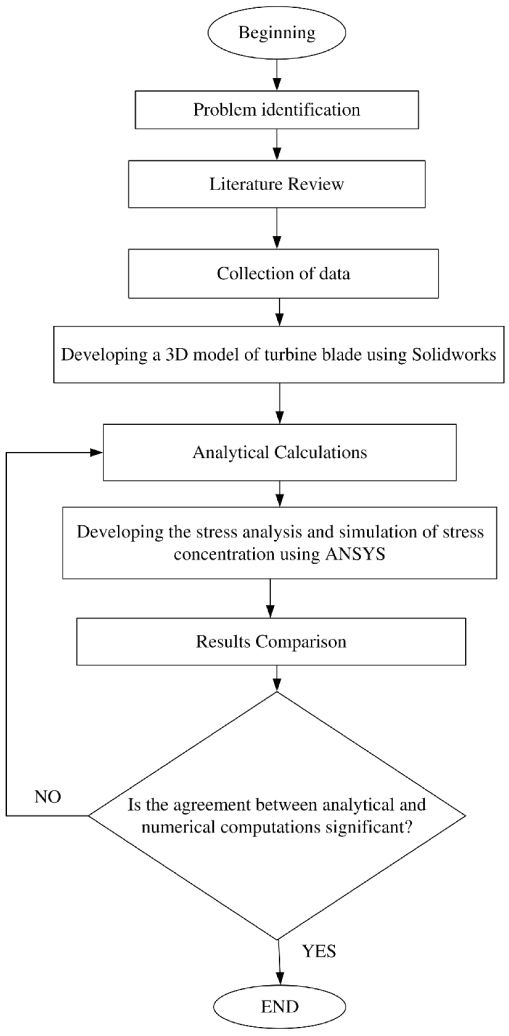

Figure 2. Implementation workflow

2.1 Steam Turbine Blade Material Characteristics, Properties and Physical Parameters

The steam turbine blade considered in this scientific work is made of INCONEL Alloy 718, a nickel-based superalloy whose mechanical characteristics are outlined in table 1 [11].

Table 1. Mechanical characteristics of INCONEL Alloy 718

Material characteristic	Value/comment
Physical density, g cm^{-3}	8,221
Melting point, ^{0}C	1380-1425
Modulus of elasticity, GPa	205
Tensile strength, MPa	869.4
Yield strength, MPa	761,2
Creep resistance	Excellent
Corrosion resistance	Excellent in air, water and steam
Oxidation resistance	Good up to 1200 ^{0}C
Wear resistance	Good
Fatigue resistance	Good

The INCONEL Alloy 718 turbine material constitutes a blend of diverse elements, each with specified percentage composition as outlined in table 2. These element compositions impart favorable characteristics, enabling the turbine to operate effectively under high-pressure steam conditions within the steam turbine system.

Table 2. Percentage composition of materials in INCONEL Alloy 718

Element	Composition , %
Nickel (Ni)	50-55
Chromium (Cr)	17-21
Iron (Fe)	18-22
Niobium (Nb)	4,75-5,5
Tantalum (Ta)	4,75-5,5
Molybdenum (Mo)	2,8-3,3
Titanium (Ti)	0,65-1,15
Aluminium (Al)	0,2-0,8
Columbium (Cb)	0,3-0,7
Others	Trace amounts

The material properties and physical parameters of the turbine blade adopted in the analysis are presented in table 3.

Table 3. Material properties and physical parameters

Material properties	Magnitude
Physical density, Kg m^{-3}	8221
Modulus of elasticity, E, MPa	$1{,}95 \cdot 10^5$
Yield strength, σ_y, MPa	761,20
Ultimate tensile strength, MPa	869,40
Elongation, %	40,00
Radius of the rotor disc, m	0,30
Height of the blade, mm	150,00
Cross-sectional area of the root of the blade, mm^2	1195,82
Blade rotation speed, ω, rad s^{-1}	314,16
Steam mass flowrate, t hr^{-1}	1602

2.2 Analytical Solution

2.2.1 Centrifugal Stress on the Turbine Blade

The rotating blades encounter centrifugal forces as a consequence of their circular motion within the turbine. These forces exert an outward pressure on the blades, directly proportional to the square of the rotational speed and the distance on the blade from the center of rotation. Considering a simplified two-dimensional (2D) representation of the blade as depicted in figure 3 [9], the centrifugal force acting on the turbine blade, denoted by F_C is calculated using equation (1).

$$F_C = m \cdot r \cdot \omega^2 \tag{1}$$

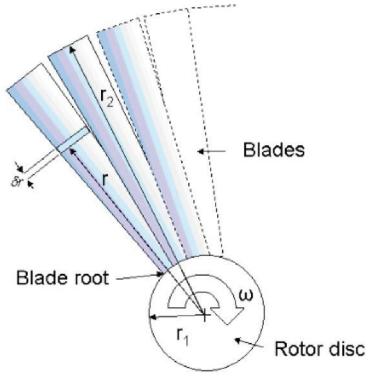

Figure 3. Load acting rotor blade

Where m is the mass of the blade, r is the radial distance from the center of rotation to the blade tip, and ω the angular velocity of the blade.
Considering an infinitesimal mass segment, denoted by δm, with a width dr, located at a distance r from the center of rotation, the centrifugal force acting on this point, represented by δF_C takes the form of equation (2).

$$\delta F_c = \delta m \cdot r \cdot \omega^2 \tag{2}$$

Given the cross-sectional area of the blade is A, mm^2, and the material physical density ρ, kg mm^{-3}, then the infinitesimal mass of the element takes the form of equation (3).

$$\delta m = \rho \cdot A \cdot dr \tag{3}$$

Substituting equation (3) into (2), and assuming that both the material physical density and the cross-sectional area are constant, we get equation (4).

$$\delta F_c = \rho \cdot A \cdot \omega^2 \cdot r \cdot dr \tag{4}$$

Integrating equation (4) from the centroid of the turbine shaft to the blade tip [10] gives the force exerted on the entire turbine blade in the form of equation (5).

$$F_C = \rho \cdot A \cdot \omega^2 \int_{r_1}^{r_2} r dr \tag{5}$$

So that the resultant centrifugal force is determined using the equation (6).

$$F_C = \rho \cdot A \cdot \omega^2 \cdot \frac{r_2^2 - r_1^2}{2} \tag{6}$$

Where r_1 is the radius of the rotor disc, and r_2 is the sum of the height of the blade and the radius of the rotor disc, as shown in figure 2.
Considering the data provided in table 3, we calculate the total radius of the blade by summing up the radius of the rotor disc (r_1 = 0,3 m) and the height of the turbine blade, so that, r_2 = 0,45 m. Substituting all the known parameters into equation (6) gives the centrifugal force on the blade, F_C = 54600 N.

2.2.2 The Centrifugal and Bending Stresses on the Turbine Blades

The centrifugal stress σ_c at the blade root is then calculated using the relation (7).

$$\sigma_c = \frac{F_c}{A_{root}} \tag{7}$$

Where A_{root} is the cross-sectional area of the blade root. So that the resulting centrifugal force acting on the blade root, σ_c = 45,50 MPa.
We must also take into account the bending stress on the steam turbine blade due to the steam pressure. This stress is sensitive to various factors, including the blade geometry, material properties, operating conditions, and the aerodynamic forces acting on the blade. On a beam-like structure, this stress takes the form of equation (8).

$$\sigma_B = \sqrt{\sigma_t^2 + \sigma_a^2} \tag{8}$$

The tangential bending stress on the blade takes the form of equation (9).

$$\sigma_t = \frac{M}{I_x} \cdot y \tag{9}$$

The axial bending stress on the blade takes the form of equation (10).

$$\sigma_a = \frac{M}{I_y} \cdot x \tag{10}$$

Where M is the bending moment due to steam pressure, x, y are the distances from the neutral axis to the outermost part of the blade in the x and y directions respectively, I_x, I_y are the

moments of inertia in the x and y directions respectively.

Formulation of the bending stress requires scrutiny of the combined velocity triangle for steam turbine illustrated in the figure 4 [12]. This is a graphical assessment of the velocity distribution of steam as it traverses through the steam turbine blade. The velocities are represented using velocity triangles, which illustrate the magnitudes and directions of various velocity components.

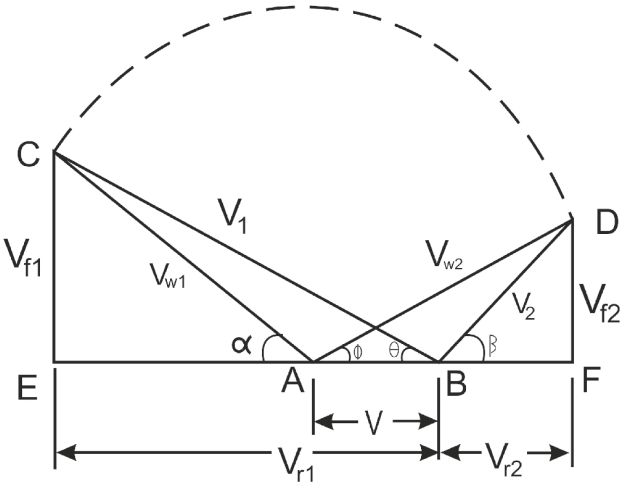

Figure 4. Combined velocity triangle for steam turbine

The free body diagram of the steam turbine blade adopted in the analysis is given in figure 5.

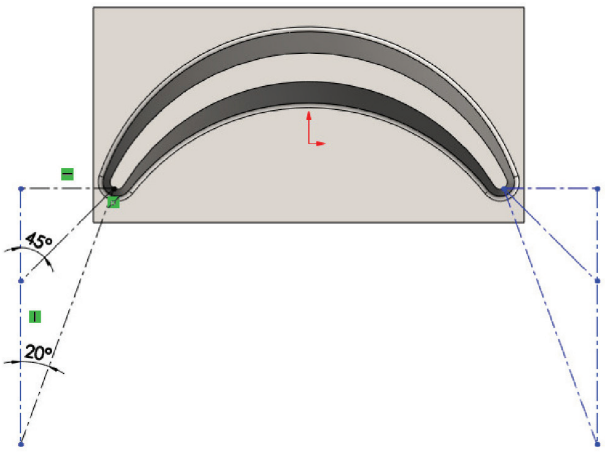

Figure 5. Steam turbine blade cross-section with velocity diagram

The mass flowrate, $\dot{M}$, associated with all the blades in a circular section of the steam turbine under scrutiny is given in table 3. The total number of turbine blades in each circular section is given as, n = 90, therefore, the mass flowrate associated with a turbine blade takes the form of equation (11).

$$\dot{m} = \frac{\dot{M}}{n} \tag{11}$$

So that, on substituting into equation (11), $\dot{M} = 4{,}94\ \mathrm{kgs}^{-1}$.

With reference to the depiction in figure 4, we generate a combined velocity triangle diagram for the steam turbine blade adopted in the analysis as shown in figure 6.

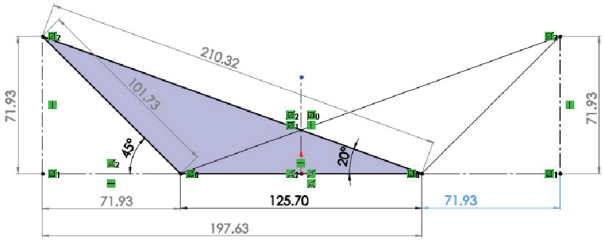

Figure 6. Combined velocity diagram of the turbine blade

The approximate values for the tangential and axial components are obtained from figure 6. The dimensional lengths correspond to relative velocities in m s^{-1}. From this figure, we retrieve the angles $\alpha = \beta = 45^0$, and $\theta = \Phi = 20^0$; representing the angle the incoming steam makes with the tangent of the wheel at the steam inlet, the angle the discharging steam makes with the tangent of the wheel at the steam outlet, the inlet angle of the moving blades, and the outlet angle of the moving blades respectively. The linear velocity V is calculated from the angular velocity of the rotor.

At the entrance, the vertical component velocity of flow V_{f1} corresponds to the axial component velocity V_1, while the velocity of flow at the exit V_{f2} aligns with the axial component V_2. Since both V_{f1} and V_{f2} are identical at a velocity of

71,93 m s^{-1}, the axial force acting on the blade becomes zero, implying that only the tangential force is exerted on the blade. From the figure 6, the velocity of the steam relative to the moving blade V_{r1} = 197,63 m s^{-1} at the inlet and the velocity of steam relative to the moving blade V_{r2} = 71,93 m s^{-1} at the outlet are used to calculate the tangential force using equation (12).

$$F_t = \dot{m}(V_{r1} + V_{r2}) \quad (12)$$

So that, the tangential force F_t = 1332,82 N.
The tangential moment M_t caused by the tangential force takes the form of equation (13).

$$M_t = F_t(r_2 - r_1) \quad (13)$$

So that M_t = 199,92 N m.

Table 4. Principal moment of inertia at the centroid, I_y and the depth of the blade from the central axis

Centroid relative to output coordinate system origin, mm		x = 0,00 y = 1,00 z = -9,11	
Moments of inertia of the area, at the centroid, mm^4	L_{xx}=74635,33 L_{yx}=0,00 L_{zx}=-24,44	L_{xy}=0,00 L_{yy}=731171,07 L_{zy}=0,00	L_{xz}=-24,44 L_{yz}=0,00 L_{zz}=656535,74
Polar moment of inertia of the area, at the centroid = 731171,07 mm^4		Angle between principal axes and part axes = 90^0	
Principal moments of inertia of the area, at the centroid , mm^4		I_x = 74635,33 I_y = 656535,74	
Moments of inertia of the area , at the output coordinate system, mm^4	L_{xx}=174679,60 L_{yx}=0,83 L_{zx}=16,86	L_{xy}=0,83 L_{yy}=830024,43 L_{zy}=-10850,11	L_{xz}=16,86 L_{yz}=-10850,11 L_{zz}=657726,64

Table 4 entails the principal moment of inertia at the centroid, I_y and the depth of the blade from the central axis. The measurements are based on sectioned model. The cross-sectional area of the selected face, A = 1190,91 mm^2. The value of the principal moment of inertia along the y-axis, I_y, and its corresponding length, y from the neutral axis is used to calculate the tangential stress by substituting these values into equation (9), so that σ_t = 50,65 MPa. Due to the fact that the axial force acting on the blade is zero, the bending stress on the turbine blade, σ_B = σ_t = 50,65 MPa.
The total stress acting on the turbine blade is determined by summing up the tangential and centrifugal stresses on the blade, equating to 96,15 MPa.

2.3 ANSYS Supported Numerical Solution

The Ansys Workbench's static structural analysis module was used in the numerical computation of centrifugal and bending stresses. This module utilizes the FEA techniques, which involve breaking down a complex structure into smaller, simpler elements. The equations governing the motion and behavior of each individual element are then solved numerically to determine the stress, strain, and displacement distributions throughout the entire structure [13]. By discretizing the problem, the program effectively analyzes the centrifugal and bending stresses acting on the blade.
The 3D model of the steam turbine blade subjected to numerical simulation is given in figure 7.

2.3.1 Meshing and Solving for Centrifugal Stress

In the static structural analysis module, the geometry file of the steam turbine blade is imported, the material properties of the blade defined, in this case, Nickel alloy INCONEL 718 is chosen from the ANSYS material database, the coordinate system for the analysis is defined, and the meshing processes initiated. The FEA technique solves the equations governing the motion of the structures on

infinitesimal volume elements of the solid domain. The meshing process divides the supplied geometry into infinitesimal elements linked by nodes. The resulting mesh is given in figure 8. The mesh element size for this analysis was chosen based on several critical factors, taking into account the distinction between critical and non-critical regions of the blade.

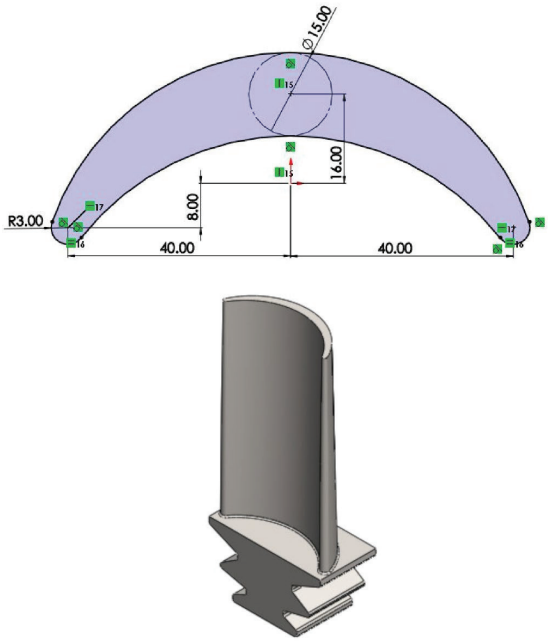

Figure 7. 3D model of the steam turbine blade adopted in the numerical solution

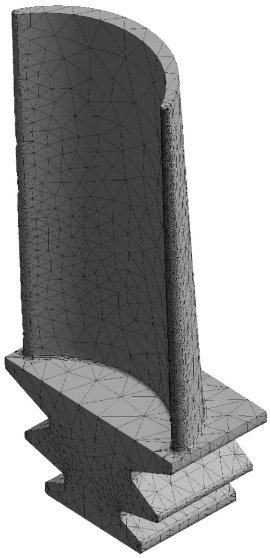

Figure 8. Steam turbine blade mesh

The blade's geometry has both simple and complex features, necessitating a variable mesh density approach, considering:

a) High stress gradient areas such as the root, trailing edge, and the leading edge of the blade, in which finer mesh elements were adopted. This facilitated accurate analysis of stress concentrations.

b) Uniform material regions such as the inner and outer arc of the blade, in which coarser mesh elements were considered. The homogeneous nature of the blade material allowed for coarser mesh in less critical areas without compromising the required accuracy.

This strategy reduced computational time and facilitated optimization on resource usage while maintaining the necessary accuracy.

The meshing process is proceeded by definition of boundary conditions on the mesh as depicted in the figure 9. This process involves applying a fixed support condition to the region where the blade attaches to the rotor disc section. Additionally, a rotational velocity of 3000 rpm is specified, which generally corresponds to the operating speed of the NPP steam turbines.

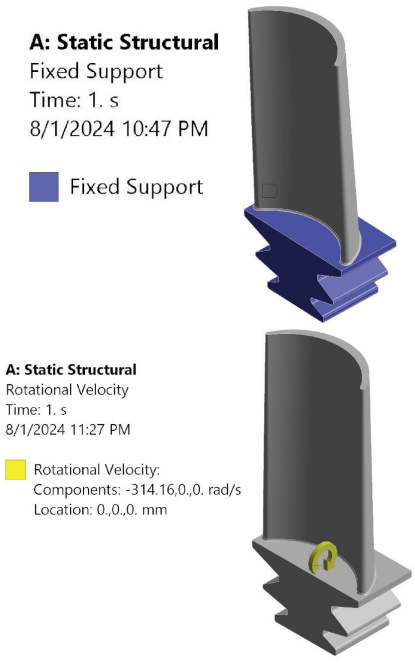

Figure 9. Boundary conditions

With the setup completed; including the material properties, coordinate system, mesh, and the boundary conditions, the Ansys static structural analysis module solution is run to evaluate the stresses and deformations on the turbine blade under the specified centrifugal loading conditions.

2.3.2 Solving for Bending Stress

Given that the simulation of steam flow using Ansys Computational Fluid Dynamics (CFD) is beyond the scope of the primary objective of this scientific work, the adopted approach in the computation of bending stress is not as straightforward as it would be if CFD is integrated in the solution. Instead of performing CFD simulation to determine the bending force acting on the blade, this value is arrived at by an analytical means. The bending force is then directly supplied as the primary bending load in the boundary conditions within the static structural analysis module. While a comprehensive CFD simulation would have provided a detailed and accurate representation of the steam-blade interaction, the adopted approach strikes a balance between computational feasibility and capturing the essential bending stress effects within the scope of the primary objective of the scientific work. The static structural module is then used to compute the bending stress in the same manner as previously executed in the case of the centrifugal stress. All the boundary conditions in this case are the same except for the bending force on the blade.

The notable difference in the boundary conditions is the introduction of the bending force acting on the blade. The analysis setup; including the geometry, material properties, coordinate system, and the mesh remain identical. Figure 10 is a depiction of the bending force applied to the turbine blade, with the fixed support constraint applied at the region where the blade attaches to the rotor section. From this we determine the equivalent force exerted by the steam jet impinging on the blade's surface.

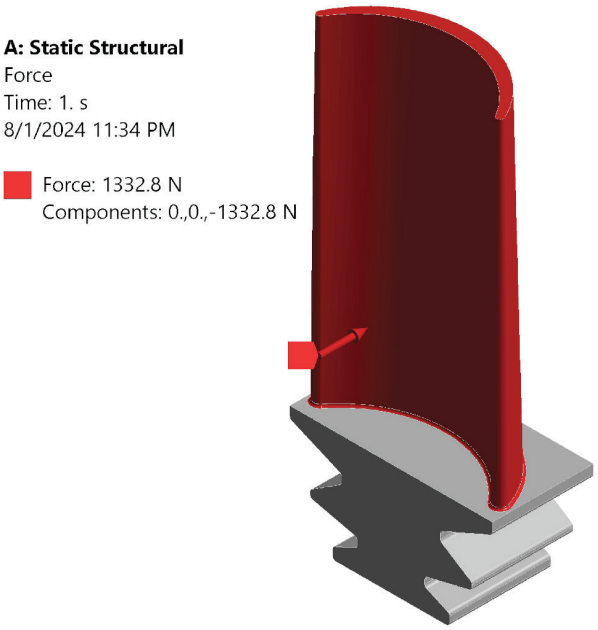

Figure 10. Equivalent force exerted by the steam jet impinging on the blade surface

3. RESULTS

Figure 11 is a depiction of the equivalent (Von-Mises) stress distribution and total deformation in the model; the results of the numerical computation of centrifugal stress. The color scale indicates the stress values, ranging from a minimum of 0,00 MPa to a maximum of 45,33 MPa. The areas with higher stress concentrations are highlighted in red and orange, while the lower stress regions are highlighted in blue and green. Figure 12 is a depiction of the bending stress and the associated total deformation force on the blade. The maximum bending stress experienced by the steam blade is 52,80 MPa. The comparison is given in the table 5.

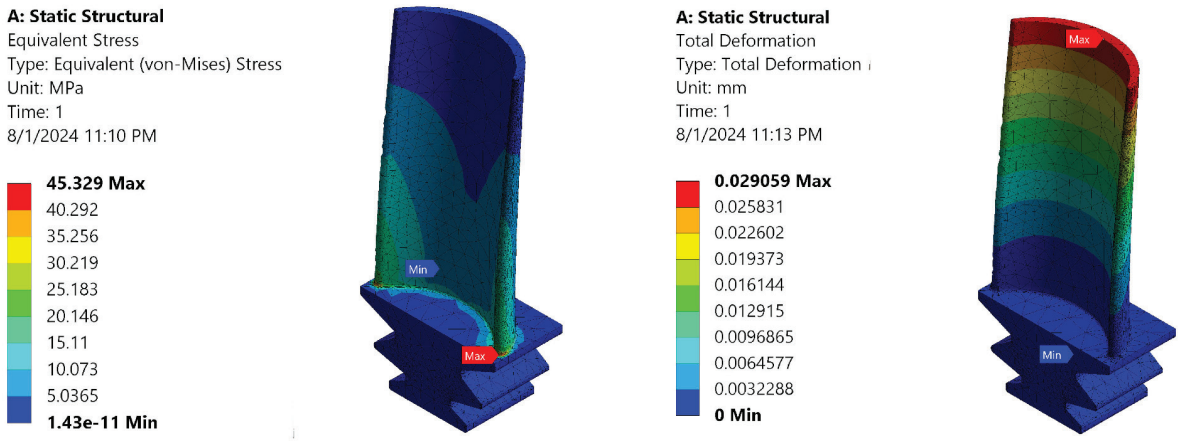

Figure 11. Centrifugal stress and associated total deformation

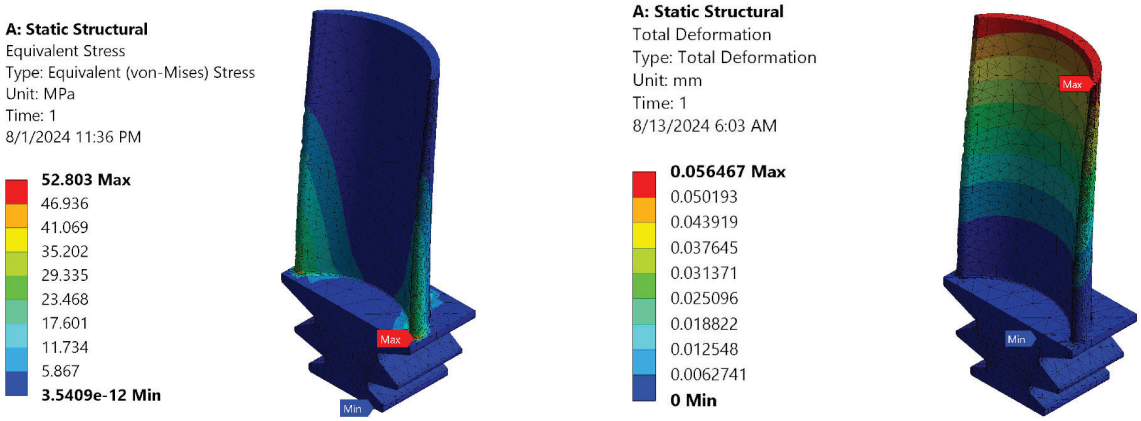

Figure 12. Bending stress and associated total deformation

Table 5. Comparison of analytical and numerical results

	Analytical	Numerical	% difference
Centrifugal stress, MPa	45,50	45,33	0,38
Bending stress, MPa	50,65	52,80	4,07
Total, MPa	96,15	98,13	2,02

CONCLUSION

The analytical technique yielded a total stress of 96,15 MPa, arrived at by summing up the centrifugal stress and bending moment stress caused by the impingement of steam jet on the blade. The total stress registered by the numerical technique is 98,13 MPa, slightly higher than the analytical results. The discrepancy in the computation of total stress by these two techniques represents 2,02% difference.

The resulting discrepancy, even though slightly significant, underscores the importance of

conducting comparative studies. While in this case the analytical method offers a simplified approach, a computational simulation provides a more comprehensive and potentially more reliable means of assessing the structural integrity and performance of the steam turbine blade under realistic operation conditions.

The difference in the results could be attributed to the limited scope of this scientific work, i.e., the decision not to incorporate the CFD analysis functionality into the static structural analysis workflow for purposes of computing the bending stress associated with the steam jet on the blade. However, the manifesting difference is one that is insignificant in the validation of the agreement between numerical and analytical computation techniques.

REFERENCES

1. **Verde C., Sánchez-Parra M.** Monitorability Analysis for a Gas Turbine Using Structural Analysis // IFAC Proceedings Volumes. – 2006.– Vol. 39, Issue 13. – P. 675-680. – ISSN 1474-6670. – DOI: 10.3182/20060829-4-CN-2909.00112
2. **Sinha, A., Swain, B., Behera, A., Mallick, P., Samal, S.K., Vishwanatha, H.M., Behera, A.** A Review on the Processing of Aero-Turbine Blade Using 3D Print Techniques // Journal of Manufacturing and Materials Processing. – 2022.– Vol. 6, Issue 1. – P. 16. – ISSN 2504-4494. – DOI: 10.3390/jmmp6010016
3. Thermal Engineering. (2019). What is Turbine Blade — Definition [online] Available at: https://www.thermal-engineering.org/what-is-turbine-blade-definition/ (Retrieved — 02/08/2024)
4. **Mingyu Zhu**. Design and Analysis of Steam Turbine Blades // Journal of Physics: Conference Series. – 2019.– Vol. 1300, Issue 1. – P. 012056. – DOI: 10.1088/1742-6596/1300/1/012056
5. Impulse Turbine and Reaction Turbine Working Principle [online] Available at: https://mechanicalengineeringsite.com/impulse-turbine-and-reaction-turbine-working-principle/ (Retrieved — 02/08/2024)
6. **Tateki Nakamura Kiyoshi Segawa Nobuhiro Isobe, Takashi Saito**. Highly-reliable Design Technology of Steam Turbine for Nuclear Power Plant, 2009
7. **Prabhunandan G.S, C., Byregowda H.V**. Static and Fatigue Analysis of a Steam Turbine Blade // International Journal of Latest Technology in Engineering, Management & Applied Science. – 2016.– Vol. 5, Issue 10. – P. 60-62. – ISSN 2278-2540
8. **Naveen kumar S., Konduru Sivaprasad Raju, Bhakiyaraja S., Vijayaganapathy D.** Static and Design Analysis of a Steam Turbine Blade // International Journal of Pure and Applied Mathematics. – 2018.– Vol. 120, Issue 6. – P. 3989-3996. – ISSN 1314-3395
9. **Anilkumar Konderu, Ganesh Purushothaman**. Determination of Thermal Stresses on Turbine Blades of Gas Turbine with NACA Airfoils by Finite Element Analysis // International Journal of Innovative Science and Research Technology. – 2017.– Vol. 2, Issue 12. – P. 393-398. – ISSN 2456-2165
10. **Swarnalata Naga Durga K., Sesha Talpa Sai P.H.V.** Design and Analysis of Steam Turbine Blade Using FEA // International Journal of Scientific Engineering and Technology Research. – 2015.– Vol. 4, Issue 29. – P. 5661-5665. – ISSN 2319-8885
11. ASM Aerospace Specification Metals Inc. – Special Metals INCONEL Alloy 718 [online] Available at: https://asm.matweb.com/search/SpecificMaterial.asp?bassnum=NINC34 (Retrieved – 02/08/2024)
12. Steam Turbine – Steam Turbine Velocity Diagram [online] Available at: https://www.mechanicaltutorial.com/steam-turbine-velocity-diagram (Retrieved — 03/08/2024)

13. Physics Forums: Science Discussion, Homework Help, Articles. (2017). Ansys Workbench Static Structural Analysis. [online] Available at: https://www.physicsforums.com/threads/ansys-workbench-static-structural-analysis.934410/ (Retrieved — 12/08/2024)

СПИСОК ЛИТЕРАТУРЫ

1. **Verde C., Sánchez-Parra M.** Monitorability Analysis for a Gas Turbine Using Structural Analysis // IFAC Proceedings Volumes. – 2006.– Vol. 39, Issue 13. – P. 675-680. – ISSN 1474-6670. – DOI: 10.3182/20060829-4-CN-2909.00112
2. **Sinha, A., Swain, B., Behera, A., Mallick, P., Samal, S.K., Vishwanatha, H.M., Behera, A.** A Review on the Processing of Aero-Turbine Blade Using 3D Print Techniques // Journal of Manufacturing and Materials Processing. – 2022.– Vol. 6, Issue 1. – P. 16. – ISSN 2504-4494. – DOI: 10.3390/jmmp6010016
3. Thermal Engineering. (2019). What is Turbine Blade — Definition [online] Available at: https://www.thermal-engineering.org/what-is-turbine-blade-definition/ (Retrieved — 02/08/2024)
4. **Mingyu Zhu**. Design and Analysis of Steam Turbine Blades // Journal of Physics: Conference Series. – 2019.– Vol. 1300, Issue 1. – P. 012056. – DOI: 10.1088/1742-6596/1300/1/012056
5. Impulse Turbine and Reaction Turbine Working Principle [online] Available at: https://mechanicalengineeringsite.com/impulse-turbine-and-reaction-turbine-working-principle/ (Retrieved — 02/08/2024)
6. **Tateki Nakamura Kiyoshi Segawa Nobuhiro Isobe, Takashi Saito**. Highly-reliable Design Technology of Steam Turbine for Nuclear Power Plant, 2009
7. **Prabhunandan G.S, C., Byregowda H.V**. Static and Fatigue Analysis of a Steam Turbine Blade // International Journal of Latest Technology in Engineering, Management & Applied Science. – 2016.– Vol. 5, Issue 10. – P. 60-62. – ISSN 2278-2540
8. **Naveen kumar S., Konduru Sivaprasad Raju, Bhakiyaraja S., Vijayaganapathy D.** Static and Design Analysis of a Steam Turbine Blade // International Journal of Pure and Applied Mathematics. – 2018.– Vol. 120, Issue 6. – P. 3989-3996. – ISSN 1314-3395
9. **Anilkumar Konderu, Ganesh Purushothaman**. Determination of Thermal Stresses on Turbine Blades of Gas Turbine with NACA Airfoils by Finite Element Analysis // International Journal of Innovative Science and Research Technology. – 2017.– Vol. 2, Issue 12. – P. 393-398. – ISSN 2456-2165
10. **Swarnalata Naga Durga K., Sesha Talpa Sai P.H.V.** Design and Analysis of Steam Turbine Blade Using FEA // International Journal of Scientific Engineering and Technology Research. – 2015.– Vol. 4, Issue 29. – P. 5661-5665. – ISSN 2319-8885
11. ASM Aerospace Specification Metals Inc. — Special Metals INCONEL Alloy 718 [online] Available at: https://asm.matweb.com/search/SpecificMaterial.asp?bassnum=NINC34 (Retrieved — 02/08/2024)
12. Steam Turbine – Steam Turbine Velocity Diagram [online] Available at: https://www.mechanicaltutorial.com/steam-turbine-velocity-diagram (Retrieved — 03/08/2024)
13. Physics Forums: Science Discussion, Homework Help, Articles. (2017). Ansys Workbench Static Structural Analysis. [online] Available at: https://www.physicsforums.com/threads/ansys-workbench-static-structural-analysis.934410/ (Retrieved — 12/08/2024)

Patrick Kiprotich Langat, 14.03.01 Nuclear Power Engineering and Thermal Physics, Bachelor's degree holder from the Institute of Nuclear Physics and Engineering, National Research Nuclear University MEPhI (NRNU MEPhI), Obninsk Institute for Nuclear Power Engineering (IATE), 249039, Kaluga Region, Obninsk City District, Obninsk, Studgorodok Territory, 1. E-mail: info@iate.obninsk.ru; ORCID: 0009-0005-6450-8692

Mariia Vladimirovna Volkova, PhD, Associate professor, Department of Nuclear Physics and Engineering, National Research Nuclear University MEPhI (NRNU MEPhI), Obninsk Institute for Nuclear Power Engineering (IATE), 249039, Kaluga Region, Obninsk City District, Obninsk, Studgorodok Territory, 1. E-mail: marissa36@yandex.ru ORCID: 0009-0005-1168-8247

Robert Folkenberg Siro, 14.04.01 Nuclear Power Engineering and Thermal Physics, Master's student of the Institute of Nuclear Physics and Engineering, National Research Nuclear University (NRNU MEPhI), 31, Kashirskoe Shosse, Moscow, 115409, Russian Federation, e-mail: sr008@campus.mephi.ru; ORCID: 0009-0008-1830-5677

Патрик Кипротич Лангат, 14.03.01 Ядерная энергетика и теплофизика, обладатель степени бакалавра Института ядерной физики и технологий, Национальный исследовательский ядерный университет МИФИ (НИЯУ МИФИ), Обнинский институт атомной энергетики (ИАТЭ), 249039, Калужская область, городской округ Обнинск, г. Обнинск, территория Студгородок, 1. Эл. почта: info@iate.obninsk.ru; ORCID: 0009-0005-6450-8692

Мария Владимировна Волкова, к.т.н., доцент, отделение Ядерной физики и технологий, Национальный исследовательский ядерный университет МИФИ (НИЯУ МИФИ), Обнинский институт атомной энергетики (ИАТЭ), 249039, Калужская область, городской округ Обнинск, г. Обнинск, территория Студгородок, 1. Эл. почта: marissa36@yandex.ru; ORCID: 0009-0005-1168-8247

Роберт Фолкенберг Сиро, 14.04.01 Ядерная энергетика и теплофизика, магистрант Института ядерной физики и технологий, Национальный исследовательский ядерный университет (НИЯУ МИФИ), 31, Каширское шоссе, Москва, 115409, Российская Федерация, E-mail: sr008@campus.mephi.ru, ORCID: 0009-0008-1830-5677